
Supporting Information

Molten salt synthesis of a single-crystal $\text{LiNi}_{0.5}\text{Mn}_{1.5}\text{O}_4$ cathode with an in-situ construction stable interface for 4.8 V-class all-solid-state batteries

Guang Sun¹, Zhenyou Song¹, Yiming Dai¹, Qian Yu¹, Qi Kang¹, Zhongqiang Wang¹, Yuwei Chen¹, Yongping Shi¹, Shixiang Qiao¹, Zuke Xiao¹ and Wei Luo^{1*}

Institute of New Energy for Vehicles, School of Materials Science and Engineering,
Tongji University, Shanghai 201804, China

*Corresponding Authors: Wei Luo, E-mail: weiluo@tongji.edu.cn

Experimental Section

Materials Synthesis

The scLNMO@Li₂MoO₄ cathode was synthesized in three steps. First, a stoichiometric amount of ammonium molybdate tetrahydrate [(NH₄)₆Mo₇O₂₄] · 4H₂O (Beijing Innochem Technology Co., Ltd) was dissolved in 20 ml of deionized water, into which 0.5 g of LNMO (Canrd New Energy Technology Corporation) was added and stirred for half an hour. The mixture was then vigorously stirred at 80 °C for 5 h until the deionized water was completely evaporated. The resulting powder was subsequently mixed with LiOH (Beijing Innochem Technology Co., Ltd) and processed through ball-milling (200 rpm) for 5 h. Then, the as-recived powder was further heated to 500 °C for 6 h and 830 °C for 12 h with a ramp rate of 3 °C·min⁻¹ in an air atmosphere.

Materials Characterization

X-ray diffraction (XRD) measurements for all materials were carried out by using an X-ray diffractometer (Bruker D8 Advance) with Cu K α radiation ($\lambda = 1.5405 \text{ \AA}$). The corresponding rietveld refinement was conducted using General Structure Analysis System (GSAS) II. The electron micrographs of powder samples were acquired by scanning electron microscopy (SEM, Zeiss G300) and transmission electron microscopy (TEM, FEI Tecnai G2 F20 TWIN). X-ray photoelectron spectroscopy (XPS, American Thermo Fisher Scientific ESCALAB 250Xi) was applied to identify the surface and depth profiling of the elemental composition (Ni 2p, Mn 2p, and Mo 3d). The etching speed utilized for scLNMO@Li₂MoO₄ powder samples were 0.5 nm s⁻¹ for the referenced Ta₂O₅. The chamber pressure was < 5×10⁻⁸ torr. The binding energy was calibrated with the C 1s peak at 284.8 eV. Sample transfer from an Ar-filled glovebox to the instrument was conducted within an air-tight box.

Assembly of ASSLBs and Electrochemical Measurements

All the solid-state cells were assembled in an argon-filled glovebox. The composite cathode mixture, consisting of LNMO, LIC, and VGCF in a 50:45:5 weight ratio, was obtained by hand-mixing for 30 min. Following that, LIC (40 mg) and LPSCl (40 mg) were sequentially added to a PEEK cylinder with diameter of 10 mm and pressed at 2 tons. Then, the as-prepared composite cathode (about 5 mg) was uniformly spread on one side of the LIC pellet and compacted at 2 tons. Finally, a bilayer of In foil (with a diameter of 10 mm and a thickness of 100 μm) and Li foil (with a diameter of 10 mm and a thickness of 50 μm) was placed on the side of the LPSCl pellet and pressed at 0.35 tons as an Li-In alloy anode to form the cells. The cells were assembled and left for 24 hours in order to ensure a homogeneous Li-In alloy anode before electrochemical testing. The applied pressure for the ASSLBs and testing temperature were fixed at 0.35 tons and 30 $^{\circ}\text{C}$, respectively. The cell was cycled between 3-4.8 V (vs. Li/Li^{+}) at a rate of 0.1 C (1 C = 145 mA g^{-1}) with a constant voltage cut-off of 3.5 mA g^{-1} at the end of charging. The galvanostatic intermittent titration technique (GITT) was performed with a 300 s charge/discharge at 0.1 C followed by 7200 s of relaxation. Both galvanostatic charge/discharge and GITT were carried out on a NEWARE (C-4008) battery tester within a voltage range of 3-4.8 V (vs. Li/Li^{+}). Cyclic voltammetry (CV) measurements were conducted on a potentiostat (Biologic VMP-3) at a scan rate of 1 mV s^{-1} over the voltage range of 3-4.8 V (vs. Li/Li^{+}). For in situ galvanostatic electrochemical impedance spectra (GEIS), a frequency range of 1 MHz to 1 Hz and an perturbation of 20 mA were chosen, and the measurements are conducted during the charging and discharging process with an equal interval time of 10 minutes.

Supplementary Figures

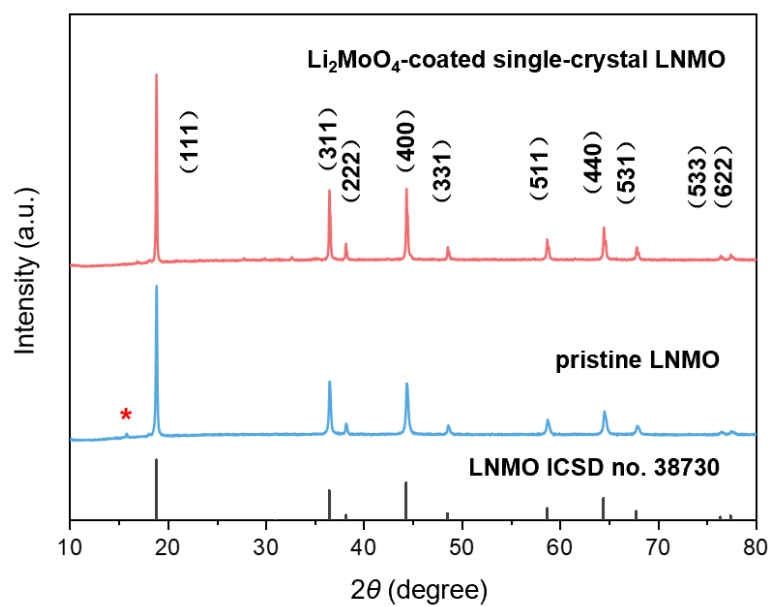


Figure S1. XRD patterns of pristine LNMO and Li_2MoO_4 -coated single-crystal LNMO.

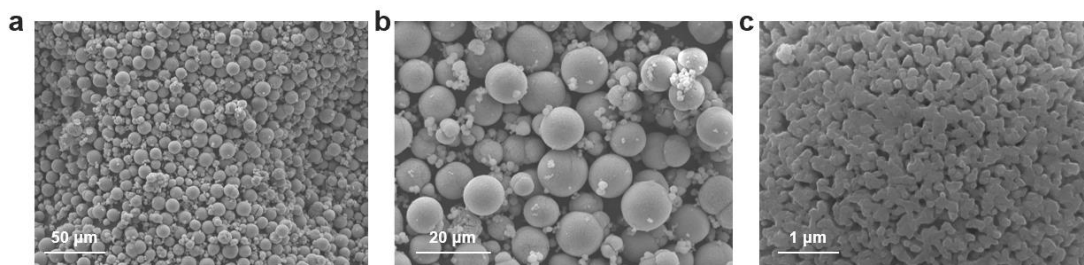


Figure S2. a-c) SEM images with different magnifications of pristine polycrystalline LNMO particles.

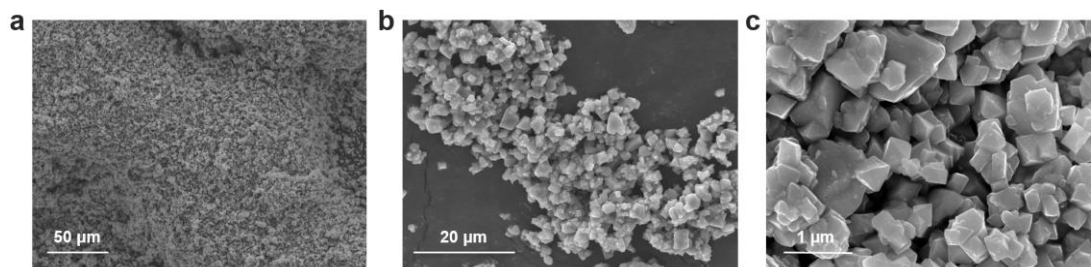


Figure S3. a-c) SEM images with different magnification of the Li_2MoO_4 -coated single-crystal LNMO particles synthesized through molten salt annealing approach using the polycrystalline LNMO particles as precursors.

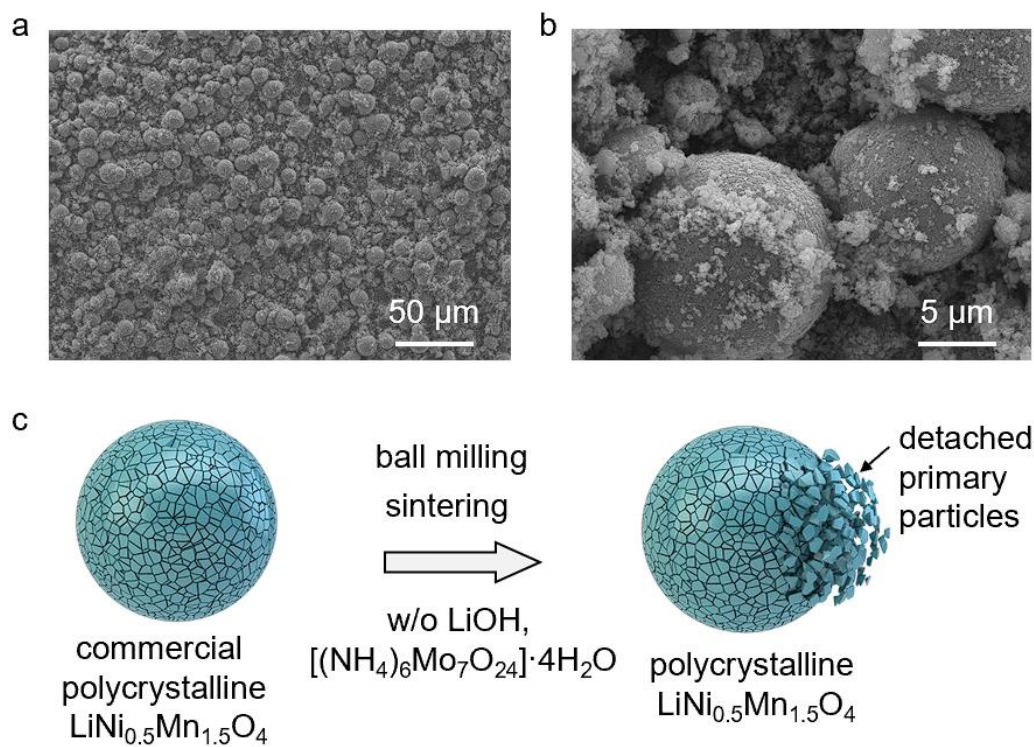


Figure S4. a, b) SEM images of the LNMO particles synthesized without LiOH and $[(\text{NH}_4)_6\text{Mo}_7\text{O}_{24}] \cdot 4\text{H}_2\text{O}$. c) Schematic illustration of the synthesized LNMO particles without LiOH and $[(\text{NH}_4)_6\text{Mo}_7\text{O}_{24}] \cdot 4\text{H}_2\text{O}$.

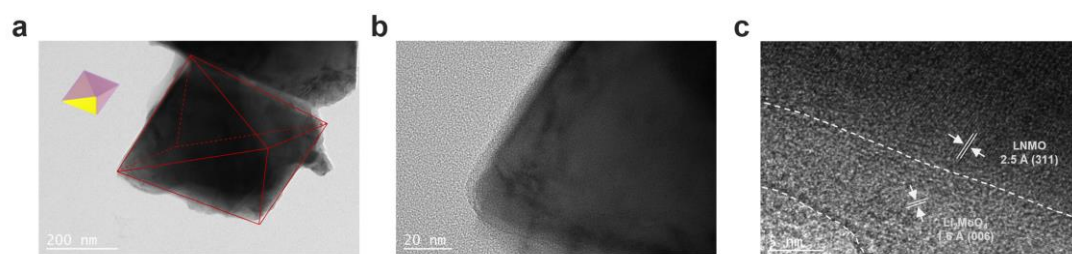


Figure S5. a, b) TEM and c) High-resolution TEM images of scLNMO@Li₂MoO₄.

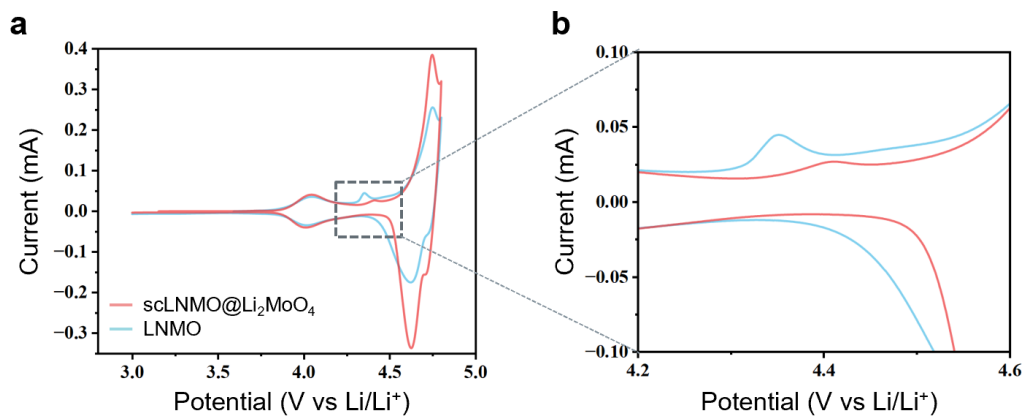


Figure S6. a) The first-cycle CV curves of the pristine LNMO and scLNMO@Li₂MoO₄ with a scan rate of 0.1 mV s⁻¹. b) Localized enlargement of the boxed portion of a).

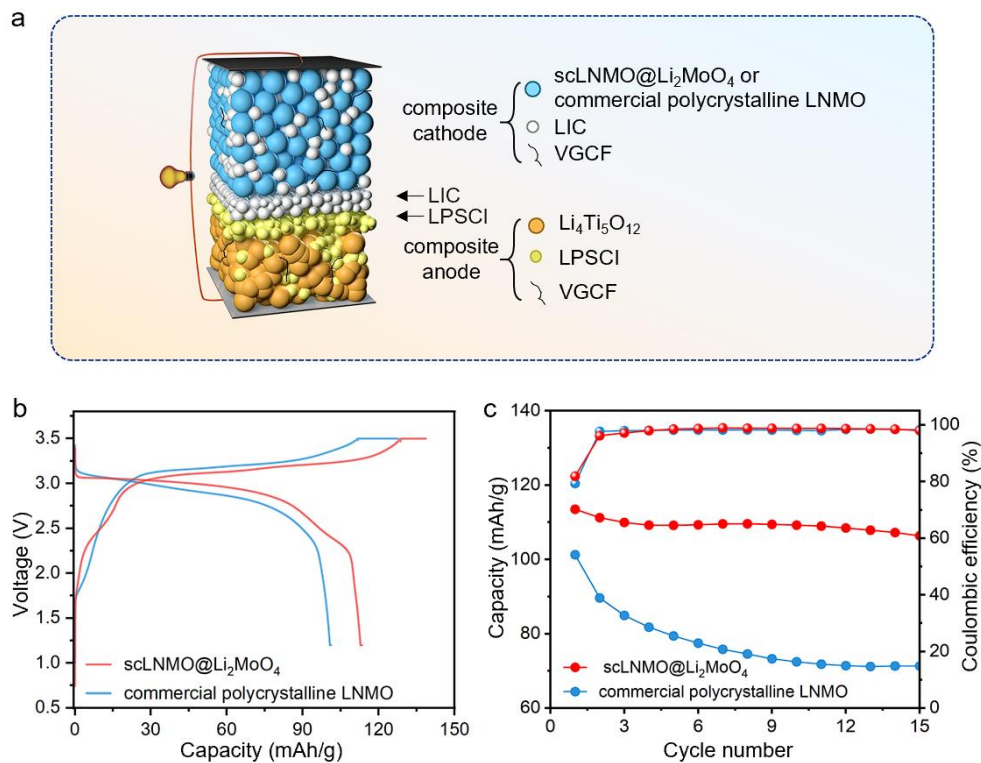


Figure S7. a) Schematic diagram of the all-solid-state full-cell configuration. b) The first charge-discharge voltage profiles and c) cycling stability of the commercial polycrystalline LNMO||LTO and scLNMO@Li₂MoO₄||LTO cells at 0.1 C.

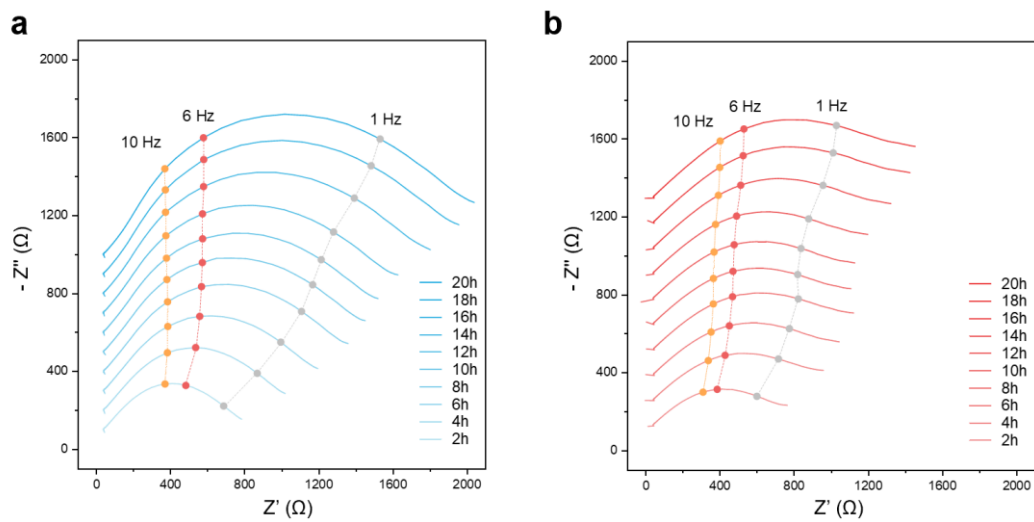


Figure S8. Nyquist plots of the a) LNMO and b) scLNMO@Li₂MoO₄ cells charged to 4.8 V in the first cycle and held for several hours.

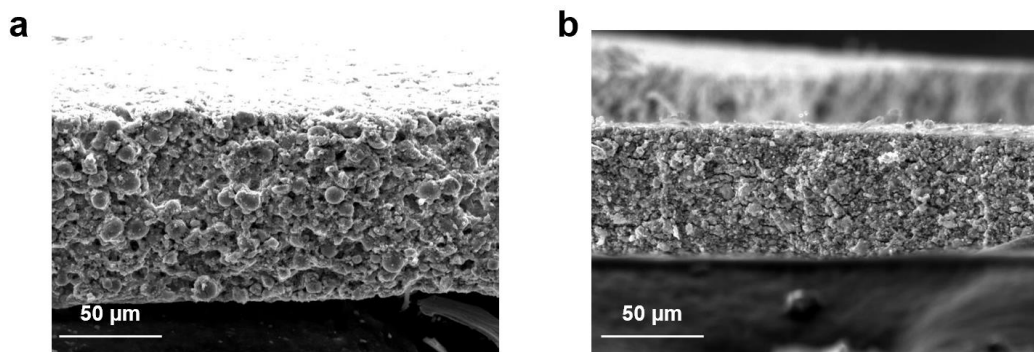


Figure S9. Cross-sectional SEM images of h) LNMO and i) scLNMO@Li₂MoO₄ composite cathodes before cycling.

Table S1. The lattice parameters of the pristine LNMO and Li₂MoO₄-coated single-crystal LNMO through Rietveld refinement analysis on XRD patterns.

Sample	Space group	a [Å]	V [Å ³]	R _{wp} [%]
LNMO	Fd $\bar{3}$ m	8.16465	544.267	3.07
scLNMO@Li ₂ MoO ₄	Fd $\bar{3}$ m	8.16860	545.058	3.29

Table S2. Summary of electrochemical test condition and performance of inorganic SEs-based ASSLBs with LNMO cathode

Cathode	SE	Specific capacity	Anode	Ref.
		[mAh g ⁻¹]/Current density		
LiNbO ₃ -coated LNMO	Li ₁₀ GeP ₂ S ₁₂	80/0.05C	Li-In	[1]
LiNbO ₃ -coated LNMO	LPSCI	115/0.1C	Li	[2]
Li ₃ PO ₄ -coated LNMO	LPSCI	49.9/0.1C	Li	[2]
Li ₄ Ti ₅ O ₁₂ -coated LNMO	LPSCI	7/0.1C	Li	[2]
Sulfurized LNMO	LPSCI	77.9 /0.1C	Li ₄ Ti ₅ O ₁₂	[3]
LiNbO ₃ -coated LNMO	Li ₃ YCl ₆	91.0/20 mA g ⁻¹	Li-In	[4]
Al ₂ O ₃ -H-LNMO (pellet type)	LPSCI	105.5/0.1C 92.4/0.2C	Li-In	[5]
Al ₂ O ₃ -H-LNMO (film type)	LPSCI	89.8/0.1C 82.1/0.2C	Li-In	[5]
Li ₃ PO ₄ - coated LNMO (Fe doped)	Li ₃ InCl ₆	94/0.05C	Li-In	[6]
scLNMO@Li ₂ MoO ₄	Li ₃ InCl ₆	128.8/0.1C	Li-In	This work

References

- 1 Oh G, Hirayama M, Kwon O, Suzuki K, Kanno R. Bulk-Type All Solid-State Batteries with 5 V Class $\text{LiNi}_{0.5}\text{Mn}_{1.5}\text{O}_4$ Cathode and $\text{Li}_{10}\text{GeP}_2\text{S}_{12}$ Solid Electrolyte. *Chem Mater*, 2016, 28: 2634–2640
- 2 Liu G, Lu Y, Wan H *et al.* Passivation of the Cathode–Electrolyte Interface for 5 V-Class All-Solid-State Batteries. *ACS Appl Mater Interfaces*, 2020, 12: 28083–28090
- 3 Wang Y, Lv Y, Su Y *et al.* 5 V-class sulfurized spinel cathode stable in sulfide all-solid-state batteries. *Nano Energy*, 2021, 90: 106589
- 4 Jang J, Chen Y-T, Deysher G *et al.* Enabling a Co-Free, High-Voltage $\text{LiNi}_{0.5}\text{Mn}_{1.5}\text{O}_4$ Cathode in All-Solid-State Batteries with a Halide Electrolyte. *ACS Energy Lett*, 2022, 7: 2531–2539.
- 5 Lee HJ, Liu X, Chart Y *et al.* $\text{LiNi}_{0.5}\text{Mn}_{1.5}\text{O}_4$ Cathode Microstructure for All-Solid-State Batteries. *Nano Lett*, 2022, 22: 7477–7483
- 6 Lee D, Cui Z, Goodenough JB, Manthiram A. Interphase Stabilization of $\text{LiNi}_{0.5}\text{Mn}_{1.5}\text{O}_4$ Cathode for 5 V - Class All - Solid - State Batteries. *Small*, 2023, 20: 2306053